THE ROLE OF Zr AND T6 HEAT TREATMENT ON MICROSTRUCTURE EVOLUTION AND HARDNESS OF AlSi9Cu3(Fe) DIECASTING ALLOY

M. Vončina [a], S. Kores [b], M. Ernecl [b], J. Medved [a]

[a] University of Ljubljana, Faculty of Natural Sciences and Engineering, Ljubljana, Slovenia
[b] Talum Tovarna aluminija d. d. Kidričevo, Slovenia

Abstract

The microstructure features and hardness of AlSi9Cu3(Fe) die casting alloy was investigated in the presence of Zr addition. The cast alloys were undergone the solutionizing treatment 2 h at 500 °C followed by artificial aging at 180 °C for 5 h. Optical microscopy and electron micro-analyzer were used to study the formation of different intermetallic phases. The hardness was tested for all samples at 25 °C. The results revealed that the intermetallic phase, based on (Al,Si)(Zr,Ti), forms when Zr is added in the investigated alloy, while the T6 heat treatment does not influence on the formation of Zr-bearing phase. Results also indicate that the hardness slightly increases in the AlSi9Cu3 alloy in as-cast state when Zr is added, while after T6 heat treatment increases by 50 % in the alloy without Zr and by 61 % in the alloy with Zr addition.

Keywords: Aluminium cast alloys; Transition metals; Solidification; Thermal analysis; Microstructure; Mechanical properties

1. Introduction

Castings of aluminium alloys are made from hundreds of different configurations of all commercial casting processes, including sand casting, the composite or permanent mould casting, precision casting, with gravity casting, low pressure and high-pressure casting for a variety of purposes [1].

The research on modification of alloys from the system Al-Si for high temperature applications are the subject of numerous studies. Gao et al. [2] investigated the impact of Zr concentration on the microstructure evolution in hypereutectic Al-Si alloy and demonstrated the concentration of Zr in these alloys can either increase or decrease the mechanical properties, depending on the morphology of formed Zr-phase. The addition of Zr must not exceed 0.2 wt. % Zr when alloying precipitation hardening Al-foundry alloys for use at high temperatures. The alloying element must fulfil four conditions [3]: it must (i) be capable of forming a strengthening phase, exhibit (ii) low solid-solubility and (iii) low diffusivity in α-Al, and (iv) retain the ability for the alloy to be conventionally solidified.

Most commercial alloys are designed so that the precipitates control the granularity of the structure.

Hardening is widely used in high strength Al-alloys. Although a number of alloys have different ratio and a combinations of alloying elements, the mechanism of hardening was the most widely studied in the Al-alloys containing Cu and Mg. Sjölander and Seifeddine [4] reported that the fine precipitates are formed during aging, and prevent the movement of dislocations and thereby increase the strength of the material. Important parameters of aged alloy are: the alloy strength, volume fraction and distribution of the precipitated phases, their mean particle sizes and the average distance between them. Some authors [4,5] proved that precipitates can effectively inhibit or hinder the movement of dislocations in α-Al matrix. Increased content of Cu, Mg and Ni and higher cooling rate of alloys from the system Al-Si-Cu-Mg improve the mechanical properties. [6] Yang et al. [7] investigated the Mg addition to Al-Si-Cu die-cast alloy and determined that Mg offered extra strengthening after the solution and ageing. θ'–Al_2Cu phase was the only phase precipitated during ageing to strengthen the Mg-free Al–Si–Cu alloys. The Mg addition introduced the Q′-AlCuMgSi precipitating phase on top of the precipitation of θ′–Al_2Cu phase during ageing, resulting in the co-operative precipitation strengthening to the alloy. Ibrahim et al.

[8] reported that the Mg and Cu, as well as the higher cooling rates improved the hardness values, especially in the T6 heat-treated condition in A319 Al-alloy. By controlling the Cu and the Cu/Mg ratio, the Al-6Si-2Cu-0.5Mg aged alloy with few primary compounds and a large number of fine Q-precipitates exhibits high strength and acceptable ductility. [9] The addition of Ni to the alloys from system Al-Si-Cu-Mg can improve the strength of the alloy by forming a δ-Al_3CuNi phase. [10] However, the tendency to form porosity which leads to a reduction in strength of the alloys is increased with increasing content of Ni.

Zr is one of the important alloying elements to improve the microstructures and properties of aluminium alloys has been claimed by Medved et al. [11]. Zhang et al. [12] reported that when Zr is added to aluminium alloys as a hardening element it may exist in four kinds of forms at different heat processing and heat-treatment stages, i.e., solid solution in matrix, coarse primary Al_3Zr phase, metastable Al_3Zr phase as well as equilibrium Al_3Zr phase. If the amount of Zr addition is too high, coarse primary Al_3Zr dendritic phases will form and aggravate the mechanical properties of the Al alloys.

Some studies [13, 14] have demonstrated that the additives Ti, V and Zr increase the tensile and compressive strength and fatigue properties of the alloys Al-Si-Cu-Mg. Yang et al. [15] have proved that the Cr in foundry alloys Al-Si modifies the β-Al_5FeSi phase, which leads to an improvement of the ultimate tensile strength of the alloy. At the alloy of the system Al-Si-Cu-Mg with micro-addition of the elements like Cr, Ti, V and Zr, the mechanical properties increase when using T6 heat treatment, while the yield stress increases by 30 % and tensile strength by 5 %, in comparison with the base alloy under the same conditions. [16] Ti/Zr/V, together with Al and Si, form a Al(ZrTiV)Si phase in the alloy A356, whereas the strength increased by 20-40 % and it shows from 11.5–15 times higher ductility compared to the commercial alloy A380. [17, 18, 19]

In the case that the alloy A354 is added 0.4 wt.% Zr and 0.2 wt. % of Ni, the microstructure is formed of an intermetallic phase $(Al,Si)_3(Zr,Ti)$ (Fig. 1), Al_3CuNi and Al_9NiFe. By raising the temperature the tensile strength of these alloys decreases as a result of increasing the proportion of Ni and Zr-phases, while at 300 °C the tensile properties (ultimate tensile strength and yield strength) are 30 % higher as compared to the base alloy. [20] The total concentration of Ni and Zr should be no greater than 0.4 wt. %. [21]

The mechanical properties of the as-cast and at heat treated condition of the alloy AlSi7Cu1Mg0.5 by the addition of Ti, V and Zr are given in Fig. 2. In such an alloy, the following phases can be formed: $Cu_{15}Al_{43}Si$, $Al_5Mg_9Si_8Cu_2$ and $Al_{14}FeMg_4Si_6$ and

intermetallic phase $Al_3Si_{26}TiV_{10}Fe$ and $Al_{13}Si_2Ti_3Zr$, wherein during the soluble annealing T6, phases $Cu_{15}Al_{43}Si$ and $Al_5Mg_9Si_8Cu_2$ dissolve, while Fe-phase AlSiCuFe and $Al_9Mg_{12}Si_6Fe$ remain undissolved. Intermetallic phases $Al_{27}SiTiZr_9$ and AlSiTiVFe remain in the microstructure in small quantities. [22]
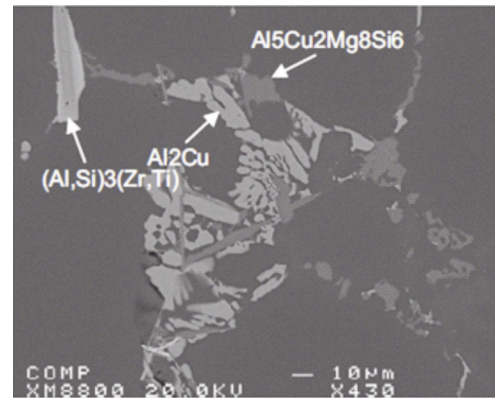

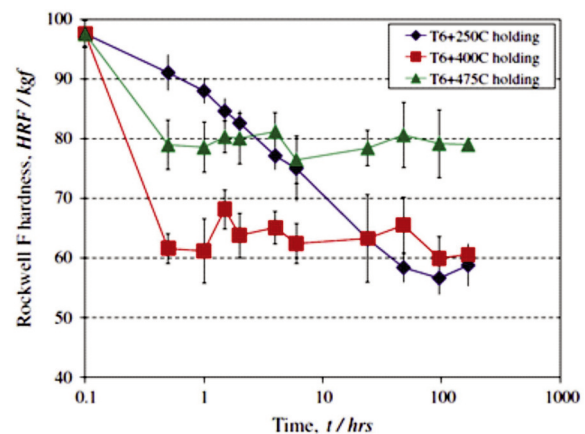**Figure 1.** *Backscattered images taken from A354 alloy with 0.4 wt.% Zr. [20]*

Figure 2. *The effect of annealing time at 250, 400 and 475 °C on hardness development for the modified alloy in the T6 condition. [21]*

The objective of this paper is to characterize the influence of Zr and heat treatment T6 on the microstructure evolution and room temperature hardness of AlSi9Cu3(Fe) die casting alloy, whereas no research was found in the available literature.

2. Experimental

Hypoeutectic AlSi9Cu3(Fe) die casting alloys without (base) and with addition of the transition element 0.2 wt.% Zr (alloyed) were investigated (Table 1). The alloy was melted in a graphite crucible inside an induction furnace. After the melt was degassed; it was purged with argon through whole

melting process, and slag was removed, 0.2 wt. % Zr was added (master alloy AlZr10) and after 15 minutes the melt was prepared for casting. The alloys were cast at a temperature of 720 °C in a Croning measuring cell, whereas the cooling rate was ~ 7 K/s and cooling curves were recorded. In order to provide and confirm the characteristic temperatures for phase precipitation, differential scanning calorimetry (DSC) was performed with 5-mm discs of 2-mm high. The DSC tests were carried out with an empty reference corundum pan, as scans in a dynamic argon atmosphere. The samples were heated up to 720 °C at 10 K/min and then equilibrated at this temperature for 10 min before cooling to room temperature at the same cooling rate at 10 K/min. The cooling rate in this case is lower as at the high-pressure die-casting process, but the influence of additives can be estimated. As-cast alloys were then subjected to T6 heat treatment, consisting of two-step solution treatment at 500 °C for 2 h, followed by water quenching and artificial aging at 180 °C for 5 h. All experimental samples for the microstructure analysis were prepared according to standard metallographic preparation (grinding and polishing) and were observed using a OLYMPUS BX61 light optical microscope, equipped with video camera DP70 AnalySIS 5.0 program. The phase characterisation was made using JEOL JSM-5610 equipped with EDS electron microanalyzer JEOL SUPERPROBE 733 with two WDS-spectrometers. Vickers hardness was tested in an as-cast and T6 heat threated samples with and without Zr addition using Micro Hardness Tester, Shimadzu, with 300 g load.

3. Results and discussion

The cooling curves and the corresponding first derivatives obtained from thermal analysis of AlSi9Cu3(Fe) and AlSi9Cu3(Fe) + Zr are shown in Fig. 3. The crystallisation region of the main phases, such as α-Al ($T_{L/min}/T_{L/max}$), (α-Al + β-Si) eutectic (T_E) and Cu-rich eutectic (T_2), can be easily observed and are marked in Fig. 1a, the characteristic temperatures are gathered in Table 2. The distinctive features between the cooling curves are the formation temperatures of the α-Al phase and the solidification time. Start of primary α-Al dendrites nucleation (T_N), which was described in detail by Ghomashchi and Nafisi [23], is marked in Fig. 1b, whereas the influence of Zr addition is clearly seen. The nucleation starts at higher temperature due to Al$_3$Zr

phase, which acts as a nucleus. The solidification time ($\Delta t_{solid.}$) is shorter and the temperature range of the solidification ($\Delta T_{solid.}$) is nearer when Zr is added to the AlSi9Cu3(Fe) diecasting alloy.

In addition to traditional thermal analysis, DSC analysis of both experimental alloys was carried out, the cooling and heating curves are presented in Fig. 4. The cooling and heating DSC curves of the base material (blue line) exhibit the same phase reactions detected by means of thermal analysis, whereas the DSC investigations of the Zr-containing alloy (green line) reveals higher liquidus temperature regarding the base alloy due to nucleation on the Al$_3$Zr phase. Because the DSC method is more accurate, two more peaks are detected; the first indicates the eutectic reaction of β-Si with Si- and Fe-bearing phases, and the second, in the last solidification region, Cu-bearing eutectics with Al$_2$Cu and Al$_5$Cu$_2$Mg$_8$Si$_6$. [24]
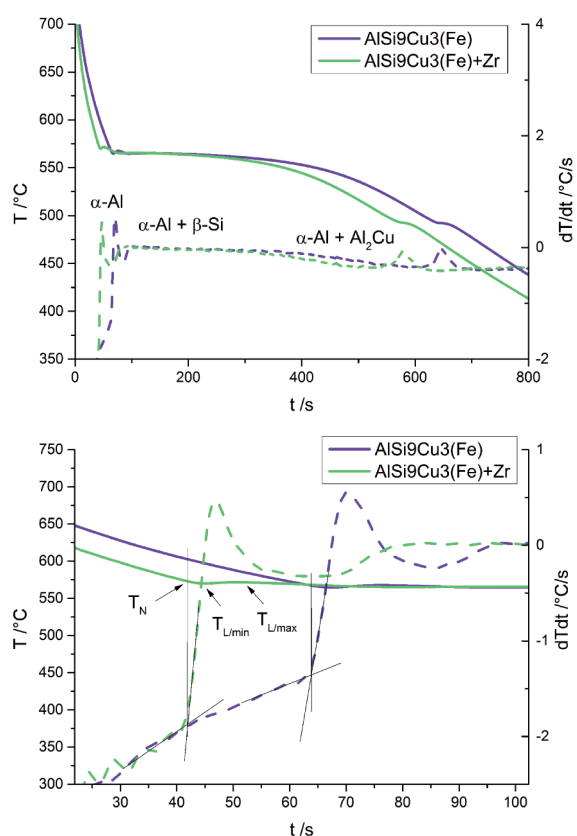

Figure 3. Cooling curve and first derivative (dotted line) of experimental AlSi9Cu3(Fe) alloys (a) and the magnification at the commencement of solidification (α-Al primary particles formation) (b)

Table 1. The chemical composition of experimental AlSi9Cu3(Fe) diecasting alloys (wt.%).

Alloy	Sn	Zr	Pb	Zn	Cu	Fe	Mn	Cr	Ti	Mg	Si	Al
AlSi9Cu3(Fe)	0.122	0.005	0.169	0.453	2.474	0.732	0.305	0.346	0.053	0.269	11.742	Bal.
AlSi9Cu3(Fe)+Zr	0.124	0.202	0.18	0.338	2.114	0.756	0.332	0.234	0.057	0.758	11.688	Bal.

The size of the peaks of last two mentioned phases are smaller when Zr is introduced to the experimental alloy, due to decreased amount of Al and Si, which were used for the formation of (Al,Si)(Ti,Zr) phase, which presumably solidifies in the first solidification region.
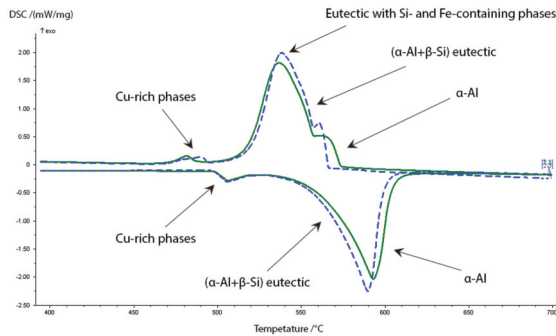

Figure 4. *Heating and cooling DSC curves obtained from of AlSi9Cu3(Fe) alloy without (blue) and with (green) Zr addition.*

The microstructure of the base alloy exhibits α-Al matrix, (α-Al + β-Si) eutectic, Al_2Cu eutectic phase, and $Al_5Cu_2Mg_8Si_6$ and $Al_{15}(FeMn)_3Si_2$ phases (Fig. 5a); in addition, small and rare Sn-Pb-rich particles (Fig. 5b) are observed in the microstructure at higher magnifications. The addition of Zr to AlSi9Cu3(Fe) alloy resulted in the formation of Zr-rich intermetallic phase (Fig. 5c and d), referred as a $(Al,Si)_3(Zr,Ti)$, as it was reported by Mohamed et al. [19] and Rakhmonov et al. [20]. In addition, these Zr-particles seems to solidify surrounded by Cu- and Fe-rich phases. These particles seems to act as heterogeneous nucleation sites for the solidification of Cu- and Fe-rich phases.

After the homogenization and aging Cu-eutectic can hardly be seen in the microstructure in both experimental alloys. When Zr is added to the alloy the morphology of Mn-eutectic changes from Chinese script to more plate-like or flaky-like (Fig. 6). After T6 heat treatment Mn-eutectic becomes like Chinese script again but it has no impact on the formation of Zr-phase, due to formation of Zr-phase in the early stage of the solidification, by means at higher temperature than T6 heat treatment.

Fig.7 illustrates the Vickers hardness of the experimental samples from AlSi9Cu3(Fe) base alloy, alloy with Zr and after T6 heat treatment. Comparison of the hardness reveals that the as-cast AlSi9Cu3(Fe) base alloy possesses the lowest hardness, whereas it

Table 2. *Characteristic temperatures of experimental alloys from thermal analysis*

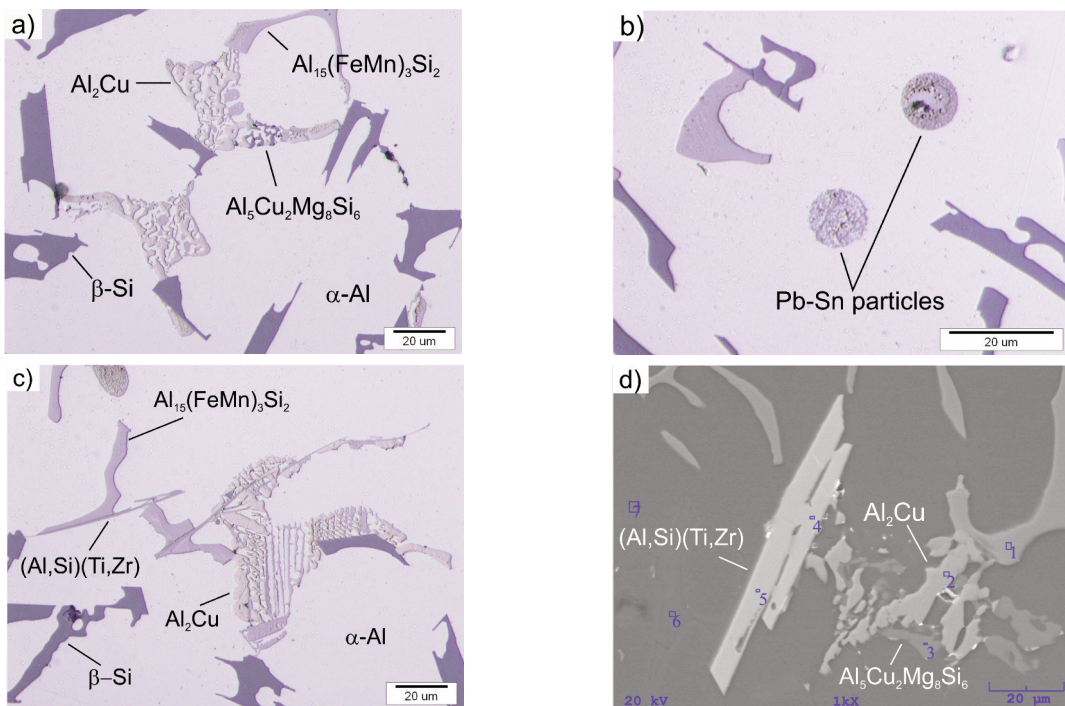| Alloy	T_N/°C	$T_{L/min}$/°C	$T_{L/max}$/°C	ΔT_L/°C	T_E/°C	T_2/°C	T_S/°C	$\Delta T_{solid.}$ /°C	$\Delta t_{solid.}$ /s
AlSi9Cu3(Fe)	567	564.7	567.6	2.9	564.7	496.1	485.7	79	610.2
AlSi9Cu3(Fe)+Zr	572.9	570	571.5	1.5	565.2	498.7	480.3	89.7	578.8

Figure 5. *Micrographs obtained from AlSi9Cu3(Fe) base alloy (a, b) and alloy with Zr (c, d), where SEM, EDS was used (d) and phases are marked.*
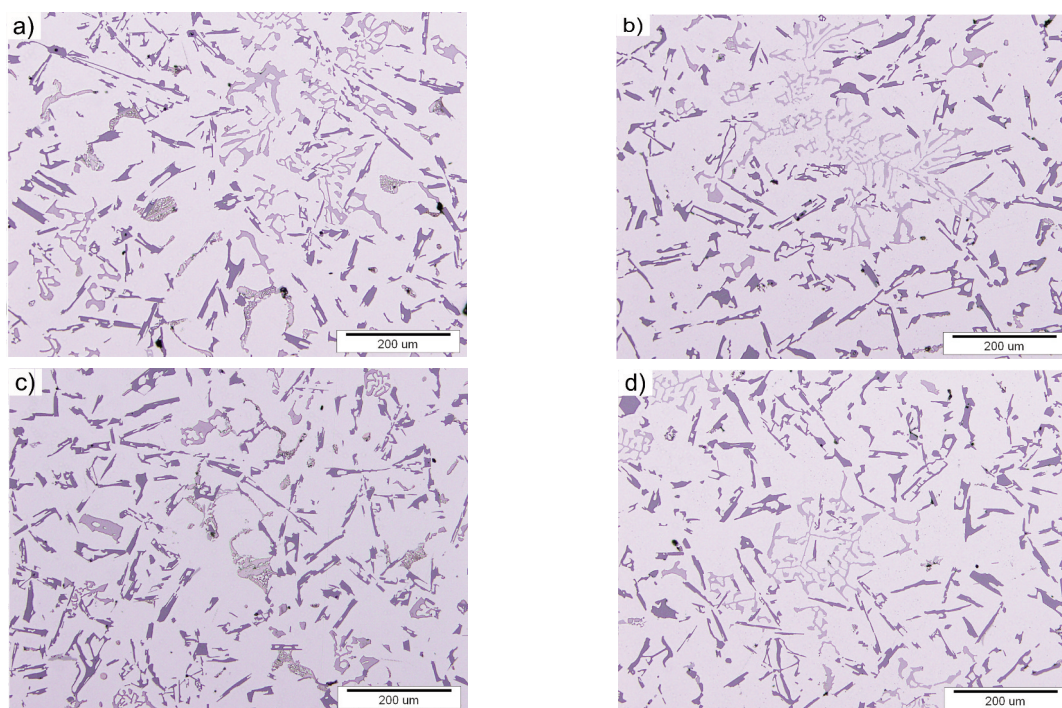
Figure 6. *Micrographs obtained from AlSi9Cu3(Fe) base alloy*
(a, b) and alloy with Zr (c, d), in as-cast state (a,c) and in T6 state (b,d).

slightly increases when Zr is added to the alloy. Zr-based phases do not have significant impact on the hardness of AlSi9Cu3(Fe) alloy at the room temperature. After the T6 heat treatment, the hardness of sample without Zr increases by 50 %, whereas the hardness of Zr containing sample increases by 61 %. This can be explained by the precipitation of Al$_3$Zr phase in α-Al.
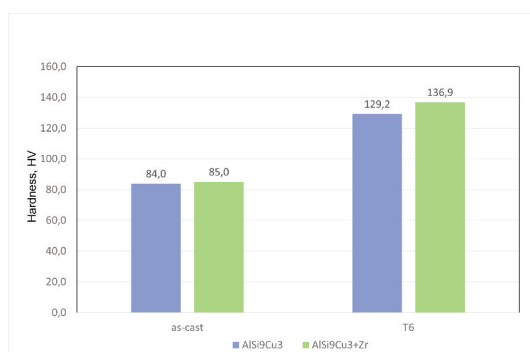

Figure 7. *Vickers hardness of investigated samples in as-cast and T6 heat treated state*

4. Conclusions

According to the literature sources and previous research about the impact of Zr on solidification, microstructure, heat treatment and mechanical properties of the Al-die casting alloys, Zr-addition presents huge potential. Following conclusions can be drawn from this study:

The addition of 0.20 wt.% Zr to AlSi9Cu3(Fe) foundry die casting alloy, leads to higher formation temperatures of the α-Al phase due to formation of Al$_3$Zr phase, which acts as a nucleus; as well as to shorter solidification time and nearer temperature range of the solidification. This conclusion were confirmed also by DSC analysis.

The addition of Zr to AlSi9Cu3(Fe) alloy resulted in the formation of Zr-rich intermetallic phase, referred as a (Al,Si)$_3$(Zr,Ti). In addition, these Zr-particles seem to solidify surrounded by Cu- and Fe-rich phases; it seems to act as heterogeneous nucleation sites for the solidification of Cu- and Fe-rich phases. In this experimental alloy, the addition of Zr changes the morphology of Mn-eutectic form Chinese script to more plate- or flaky-like and changes back to Chinese script when T6 heat treatment is introduced. Cu-eutectic can hardly be seen after T6 in both experimental alloys. T6 heat treatment has no impact on the formation of Zr-phase, due to formation of Zr-phase in the early stage of the solidification, by means at higher temperature than T6 heat treatment.

The addition of 0.20 wt.% Zr does not impact significantly on the hardness of AlSi9Cu3(Fe) diecasting alloy in as-cast state, whereas the combination of Zr-addition and T6 heat treatment have major impact on the hardness; it increases for 61

% in comparison with the base alloy, where the hardness increases for 50 %.

Acknowledgements

References

[1] D.M. Stefanescu, ASM HandBook, Volume 15 – Casting, 9th Edition, 1988.

[2] T. Gao, X. Zhu, Q. Sun, X. Liu. J. Alloy. Compd. 567 (2013) 82–88.

[3] K.E. Knipling, Development of a Nanoscale Precipitation-strengthened Creep resistant Aluminum Alloy Containing Trialuminide Precipitates. Northwestern University, Evanston, IL, 2006.

[4] E. Sjölander, S. Seifeddine, J. Mater. Process. Technol. 210 (2010) 1249–1259.

[5] E. Sjölander, S. Seifeddine, Mater. Sci. Eng.: A 528 (2011) 7402–7409.

[6] B. Jordović, B. Nedeljković, N. Mitrović, J. Živanić, A. Maričić, J. Min. Metall. Sect. B-Metall. 50 (2) B (2014) 133 - 137

[7] H. Yang, S. Ji, W. Yang, Y. Wang, Z. Fan, Mater. Sci. Eng.: A 642 (2015) 340–350.

[8] M.F. Ibrahim, E. Samuel, A.M. Samuel, A.M. Al-Ahmari, F.H. Samuel, Mater. Des. 32 (2011) 2130–2142.

[9] Y. Zheng, W. Xiao, S. Ge, W. Zhao, S. Hanada, C. Ma, J. Alloy. Compd. 649 (2015) 291–296.

[10 A.R. Farkoosh, M. Javidani, M. Hoseini, D. Larouch, M. Pekguleryuz, J. Alloy. Compd. 551 (2013) 596–606.

[11] J. Medved, S. Kores, P. Mrvar, A. Križman, M. Vončina, Livarski vestnik, vol. 63 (2016) 29–36.

[12] J.-C. Zhang, D.-Y. Ding, W.-L. Zhang, S.-H. Kang, X.-L. Xu, Y.-J. Gao, G.-Z. Chen, W.-G. Chen, X.-H. You, Trans. Nonferrous Met. Soc. China 24 (2014) 3872−3878.

[13] S.K. Shaha, F. Czerwinski, W. Kasprzak, J. Friedman, D.L. Chen, International Journal of Fatigue. 70 (2015) 383–394.

[14] S.K. Shaha, F. Czerwinski, W. Kasprzak, D.L. Chen, J. Alloy. Compd. 593 (2014) 290–299.

[15] Y. Yang, S.-Y. Zhong, Z. Chen, M. Wang, N. Ma, H. Wang, J. Alloy. Compd. 647 (2015) 63–69.

[16] S.K. Shaha, F. Czerwinski, W. Kasprzak, J. Friedman, D.L. Chen, Mater. Sci. Eng.: A 652 (2016) 353–364.

[17] S.K. Shaha, F. Czerwinski, W. Kasprzak, J. Friedman, D.L. Chen, Mater. Des. 83 (2015) 801–812.

[18] S.K. Shaha, F. Czerwinski, W. Kasprzak, D.L. Chen, Mater. Des. 59 (2014) 352–358.

[19] S.K. Shaha, F. Czerwinski, W. Kasprzak, J. Friedman, D.L. Chen, J. Alloy. Compd. 615 (2014) 1019–1031.

[20] A.M.A. Mohamed, F.H. Samuel, S.A. Kahtani, Mater. Sci. Eng.: A 577 (2013) 64–72.

[21] J. Rakhmonov, G. Timelli, F. Bonollo, Mater. Characterization 128 (2017) 100–108.

[22] W. Kasprzak, B. Shalchi, M. Amirkhiz Niewczas, J. Alloy. Compd. 595 (2014) 67–79.

[23] R. Ghomashchi, S. Nafisi, Journal of Crystal Growth. 458 (2017) 129–132.

[24] G. Timelli, S. Capuzzi, A. Fabrizi, J. Therm. Anal. Calorim. 123 (2016) 249–262.